J. Micromech. Microeng. **22** (2012) 065014 (8pp) doi:10.1088/0960-1317/22/6/065014

A novel micropreconcentrator employing a laminar flow patterned heater for micro gas chromatography

W-C Tian[1,2,3], T H Wu[4], C-J Lu[5], W R Chen[5] and H J Sheen[4]

[1] Department of Electrical Engineering, National Taiwan University, Taipei 106, Taiwan, Republic of China
[2] Graduate Institute of Electronics Engineering, National Taiwan University, Taipei 106, Taiwan, Republic of China
[3] Graduate Institute of Biomedical Electronics and Bioinformatics, National Taiwan University, Taipei 106, Taiwan, Republic of China
[4] Institute of Applied Mechanics, National Taiwan University, Taipei 106, Taiwan, Republic of China
[5] Department of Chemistry, National Taiwan Normal University, Taipei 116, Taiwan, Republic of China

E-mail: wctian@cc.ee.ntu.edu.tw

Received 30 December 2011, in final form 6 March 2012
Published 17 May 2012
Online at stacks.iop.org/JMM/22/065014

Abstract
A simple micromachined process based on one photomask is developed for a novel micropreconcentrator (μPCT) used in a micro gas chromatograph (μGC). Unique thick silver heating microstructures with a high surface area for microheater of μPCT are fabricated by combining the microfluidic laminar flow technique and the Tollens' reaction within a microchannel. Silver deposition using this laminar flow patterning technique provides a higher deposition rate and easier microfabrication compared to conventional micromachined technologies for thick metal microstructures (>200 μm). An amorphous and porous carbon film that functions as an adsorbent is grown on microheaters inside the microchannel. The μPCT can be heated to >300 °C rapidly by applying a constant electrical power of ~1 W with a heating rate of 10 °C s^{-1}. Four volatile organic compounds, acetone, benzene, toluene and xylene, are collected through the proposed novel μPCTs and separated successfully using a 17 m long gas chromatography column. The peak widths at half height (PWHHs) of the four compounds are relatively narrow (<6 s), and the minimum PWHH of 3.75 s is obtained for acetone. The preconcentration factors are >38 000 for benzene and toluene.

1. Introduction

Gas chromatography (GC) is widely used to analyze compounds in gas samples for various applications, such as indoor air quality monitoring, environmental analysis [1] and medical diagnoses [2–4]. Numerous research groups have attempted to miniaturize a GC system to facilitate a portable instrument to improve the time resolution and reduce the analytical costs of these applications [5–7]. However, the key micro components in these portable instruments, that is, preconcentrators, GC columns and online detectors, are rather complex to fabricate and require state-of-the-art equipments for implementation [8, 9]. Thus, a simple and cost-effective process for fabricating these micro components would significantly enhance the development of analytical microsystems. Therefore, this study proposes a novel fabricated micropreconcentrator (μPCT) based on this goal.

A μPCT performs as the front-end device of a μGC to collect and preconcentrate trace compounds in a test sample or environment. The target compounds are adsorbed onto adsorbents in the microchannels, and then desorbed by a heat pulse. In conventional preconcentrator heater designs, a capillary tube coiled with a metal wire is used as a heater [10]. However, with the development of microelectromechanical system (MEMS) technologies, the preconcentrator has been microfabricated and integrated into a miniaturized gas chromatograph system [11]. High-aspect-ratio structures, such

as 3D micropillar arrays, are designed and fabricated inside μPCTs to increase the internal surface area [12]. Typically, commercial carbon adsorbents with high porosity, such as Carbopack X, are packed inside the microfluidic channel for vapor collection [13, 14]. Porous silicon is then etched onto the inner surface of the microchannel to enhance adhesion between the carbon powders and substrates [15].

A high-performance microheater in a μPCT is crucial for heating adsorbent material and thermally desorbing volatile organic compounds (VOCs). Microheaters are also required in various MEMS devices, such as sensors [16–20], chemical reactors [21–23] and pneumatic pumps [24, 25]. Metallic thin films that use e-beam evaporator and sputter deposition are employed to fabricate microheaters [26]. Highly doped polysilicon is also employed as microheater material using CMOS technology [27–29]. The fabrication processes of the conventional microheaters are extremely complex and require multiple photomasks, such as those that define microfluidic channels, electrical interconnects and microheating elements with a high surface area [9]. A novel μPCT with self-heating adsorbents was presented recently [30]. Self-heating adsorbents are composed of porous gold layers, which serve as both adsorbents and heaters, and are formed at the substrate during seedless electroplating.

This study presents a novel μPCT that uses microfluidic laminar flow patterning to form thick and high-surface-area microheaters, followed by integrated adsorbent formation. A silver microheater was fabricated inside a microchannel at the liquid–liquid interface of two reactive solutions using laminar flow patterning [31, 32]. This method was applied to deposit thick silver microstructures as microheaters for μPCT, without additional photomasks. Aqueous carbohydrate was injected into the μPCT and then carbonized at a high temperature to form the adsorbent film. The design, laminar flow patterning technology developments, and characteristics of these μPCTs are discussed below.

2. Experiments

2.1. Design of micropreconcentrators

A μPCT with four liquid ports and two gas ports was designed as shown in figure 1. The dimensions of the adsorption area were 10 mm long, 1 mm wide and 200 μm deep. To increase the surface area for sample collection, cylindrical obstacle arrays with a diameter of 100 μm were arranged in the sample collection region. The configuration of these four liquid ports was used to construct five liquid streams in a microchannel. Therefore, four liquid–liquid interfaces could be obtained using laminar flow patterning to form thick microheating elements with a high surface area that function as a microheater. After the microheater was completed, the chip was diced using the dicing line and an electrical port was opened. This open port and another electrical port on the other side of the μPCT were used as the contact points between the silver microheaters and external platinum wires. The fluidic interconnect is implemented through two microfluidic ports. The μPCT is connected with a part of a μGC using fused silica tubing, as shown in figure 1. The μPCTs were composed of microchannels, microheaters and adsorbent materials. The fabrication processes are shown in figure 2.

2.2. Silicon microchannel fabrication

A p-type silicon wafer (1 0 0) with a thickness of 500 μm (SILTRONIX, France) was used as the substrate of μPCT. Only one photomask without alignment was required for optical lithography to transfer the patterns of the microchannels and micropillars on the silicon wafer, as shown in figure 2(*a*). The photoresist SPR220 (Shipley Company, MA, USA) was used as a passivation layer when an inductively coupled plasma (MESC Multiplex ICP, STS, UK) etcher was used for the etching process. The Bosch process, including the etching and the passivation cycles, was employed to etch structures with high aspect ratios [33]. In this study, the etching cycle lasted for 11.5 s. An O_2 flow of 13 sccm and an SF_6 flow rate of 130 sccm were used. A source power of 600 W and a bias voltage power of 11.5 W were applied. For the passivation cycle, a passivation layer was deposited for 7 s and a C_4F_8 flow rate of 85 sccm was supplied. A source power of 600 W with no bias voltage power was applied during the passivation process. After optimizing and characterizing the dry etching conditions, vertical microchannels and micropillar arrays were obtained, as shown in figure 2(*b*).

The etched silicon wafer was bonded to a glass plate (Pyrex 7740, Corning, NY, USA) using electrostatic force during the anodic bonding process. The electrical potential of 800 V was applied to form a thin oxide layer between the silicon wafer and Pyrex glass at 400 °C. After the silicon and glass cover were anodic bonded, the microchannels were formed, as shown in figure 2(*c*).

2.3. Silver microheater deposition

Tollens' reaction (silver-mirror reaction) was used to deposit silver wires as the heating elements for microheaters of the μPCT. Three parameters, the chemical reagent concentration, the deposition temperature and the pH value, dominate the rate of Tollens' reaction. The reaction rate can be accelerated by increasing the values of the three parameters. If the reaction rate is low, deposition of the reduced silver on the substrate surface against the shear force in a liquid stream becomes difficult. By contrast, a higher reaction rate indicates greater instability of deposition inside the microchannels. The rate of Tollens' reaction should be optimized to achieve high-quality deposition of the microheaters. In our experiment, the ammoniacal silver nitrate solution and reduction solution were prepared as follows: a 0.5 M silver nitrate solution was prepared by dissolving 0.17 g of silver nitrate (Showa Chemical Industry, Japan) in 15 to 25 mL of deionized water. Then, 14.5 M of aqueous ammonia (Shimakyu's Pure Chemicals, Japan) was added gradually to the silver nitrate solution until the precipitate dissolved and the solution became transparent. A potassium hydroxide (KOH) solution of 45% (w/w) (Shimakyu's Pure Chemicals, Japan) was added to adjust the pH value of the ammoniacal silver nitrate solution

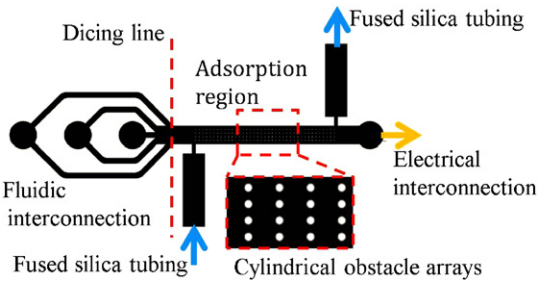

Figure 1. An illustration of the μPCT with the cylindrical obstacle array in the adsorption region and fluidic/electrical ports.

between 9 and 10. The reduction solution was created using 0.27 M of glucose (Chiabao, Taiwan) in deionized water.

A 0.1 M sensitizing solution was prepared by dissolving 2 g of stannous chloride (Nihon Shiyaku Industries, Japan) in 100 mL of 1 M diluted hydrochloric acid (Shimakyu's Pure Chemicals, Japan). The microchannels were pretreated using a stannous chloride solution for 2 min and then washed with deionized water to enhance the adhesion of the silver wires on the substrate. To form Tollens' reaction, ammoniacal silver nitrate and a reducing solution (glucose) were used. The two chemical solutions were injected separately into the multiple Y-junction microchannels to generate multiple parallel laminar flows. The $Ag^{+}_{(aq)}$ was reduced to $Ag_{(s)}$ and formed a solid metal microheater at the liquid–liquid interface inside the microchannel, as shown in figure 2(*d*).

As the liquid streams flow through the cylindrical obstacle array, silver is deposited on the inner surface of the microchannel at the liquid–liquid interfaces and side walls of the cylindrical obstacle arrays, as shown in figure 3(*a*). Before implementing electrical interconnection and adsorbent formation, the section of multiple Y-junctions was severed to reduce thermal mass. The two liquid ports were then sealed and filled with high-temperature conductive liquid paste (Shenzhen Octopus Technology, China) to serve as the electrical contact points.

2.4. Integrated carbonized adsorbent formation

Instead of packing the commercial carbonized adsorbent materials into the μPCT manually [9], adsorbent material was created using the flow through coating and pyrolysis method.

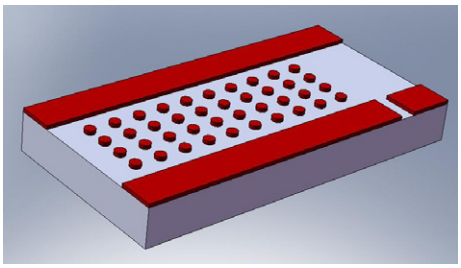

Photolithography to define the patterns on the silicon wafer

(*a*)

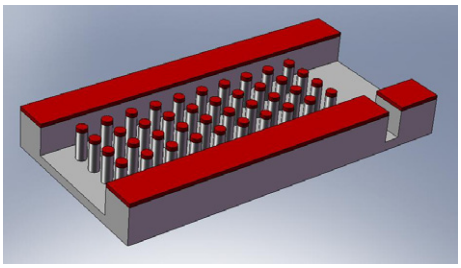

Silicon etching using DRIE to fabricate the microchannel

(*b*)

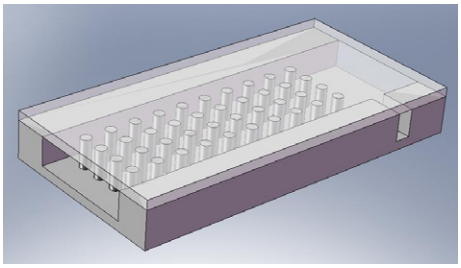

Silicon wafer anodically bonded with Pyrex glass

(*c*)

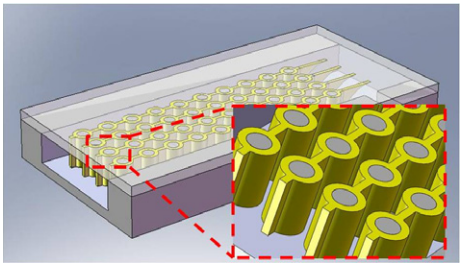

Silver microheaters formation using laminar flow patterning

(*d*)

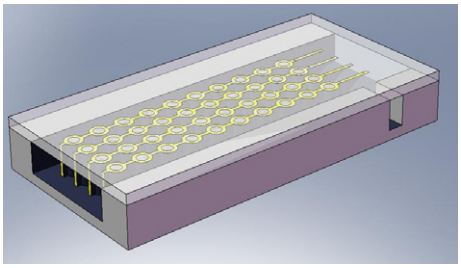

Adsorbent materials formation through pyrolysis process

(*e*)

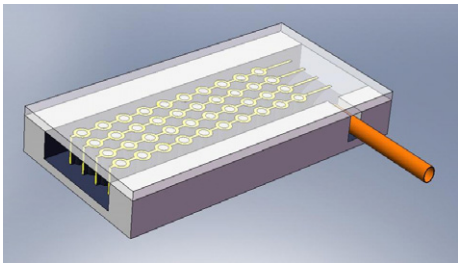

Insert fused silica capillary tubing for fluidic interconnects

(*f*)

Figure 2. Fabrication processes of the preconcentrator using the MEMS fabrication process and laminar flow patterning.

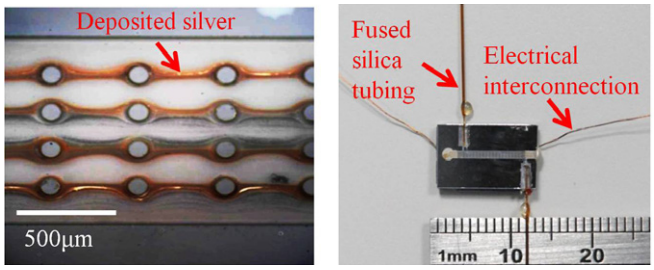

(*a*) (*b*)

Figure 3. Photo images of (*a*) the cylindrical obstacle arrays surrounded by four parallel silver wires and (*b*) the complete μPCT with electrical interconnection and fused silica capillary tubing.

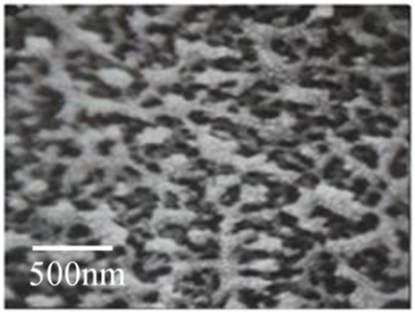

Figure 4. SEM image of porous carbon adsorbent with a surface area of 308 m^2 g^{-1} formed by the pyrolysis process of the cellulose.

The cellulose aqueous solution of 2.4% (w/w) was injected into the microchannel for 20 s. A thin cellulose film was coated on the inner wall of the microfluidic channels and silver heating elements. The carbonized temperature of the adsorbent film was characterized based on the adsorption capability of the adsorbent film. With the carbonized temperature below 500 °C and an annealing time of 2 h (in addition to 6 h of rising time from room temperature), the adsorbent film was not fully carbonized so the adsorption capacity is poor. At the carbonized temperature above 550 °C with the annealed time of 2 h, the adsorbents were fully carbonized and showed a sufficient adsorption capacity. The adsorption capacity was not varied significantly for the adsorbent film prepared at 550 °C or above. Therefore, the carbonized temperature at 550 °C with the annealing time of 2 h was chosen. An SEM image of the carbonized carbohydrate is shown in figure 4. The SEM picture was taken on another substrate which was a flat and clean silicon wafer and carbonized adsorbent film was formed using the same process as for μPCTs. The surface area of the carbonized thin film, measured by the BET method, is 308 m^2 g^{-1}. The weight of the carbonized thin film was approximately 0.3 mg, which provides a sufficient adsorption capacity for this experiment according to the results of a previous investigation using similar carbon adsorbents, such as Carbopack X [8, 9]. The weight of the carbonized film was determined by comparing the weight of the μPCT before and after the adsorbent forming process using a high-resolution balance scale (GT480, OHAUS, USA). The adsorbent film was not conformal due to the complicated microstructures inside the microchannel. Hence, the thickness of the adsorbent film was not constant inside the microchannel. In addition, the adsorbent surface area and mass are much more important parameters than the film thickness because these two parameters determine the overall adsorbent capacity.

The electrical resistance value of the silver microheaters changed slightly (from ∼8 to ∼10 Ω) after the high-temperature treatment during the pyrolysis process. The completed μPCT connects the microheater to the external

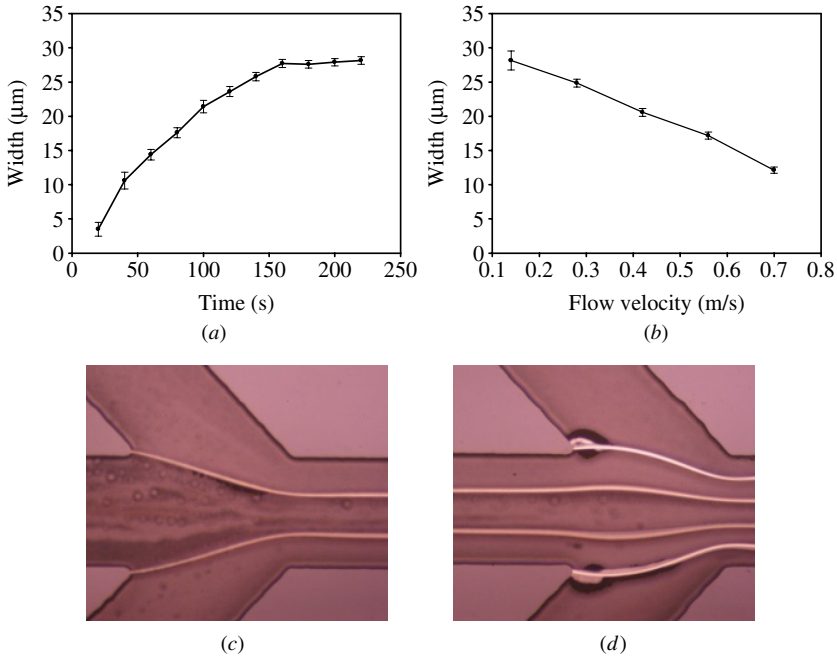

(*a*) (*b*)

(*c*) (*d*)

Figure 5. The width variations of deposited silver with (*a*) an applied flow velocity of 0.14 m s^{-1} at various deposition times and (*b*) various applied flow velocities at deposition time of 15 min; the images of silver deposition with (*c*) two and (*d*) four liquid–liquid interfaces using multiple Y-junction microchannels (microchannel width 500 μm).

Pt wires electrically and connects the microfluidic port to the fused silica capillary tubing fluidically, as shown in figure 3(*b*).

2.5. Test of organic vapor preconcentrations

A GC system (HP, USA) with a flame ionization detector (FID) was employed to characterize the desorption performance of the μPCT. Four VOCs acetone, benzene, toluene and xylene were prepared at a concentration of 10 parts per million for adsorption/desorption tests. The μPCT was connected to a six-way switching valve. This valve was switched between sampling and desorption of the four compounds to detecting GC-FID. The compound mixture was carried through the μPCT at an air flow of 1.6 mL min^{-1} for 600 s, drawing a total volume of 16 mL. After the sampling process was completed, the μPCT was heated to the desorption temperature of 300 °C for 90 s. The applied power was adjusted using an IR camera (FLIR SC325, FLIR, USA) to confirm the device temperature. A heating rate of 10 °C s^{-1} can be achieved by applying a constant electrical power of ∼1 W. The concentrated mixture was released from the adsorbent by the nitrogen carrier gas at a flow rate of 2.75 mL min^{-1} after the desorption temperature was achieved, separating a 17 m long fused silica capillary column. During the separation cycle, the initial temperature of the GC oven was set to 70 °C for 2 min and then increased to a final temperature of 150 °C, with an average heating rate of 35 °C min^{-1}.

3. Results and discussion

3.1. Characterization of laminar flow patterning

The width of the silver microheater increased only slightly from upstream to downstream because of the constant flow resistance throughout the microchannel within the first 10 mm. Variation of the silver microheater width along the fluid stream with a velocity of 0.14 m s^{-1} can be ignored (from 28 to 28.5 μm). To analyze the characteristics of the deposited silver microheater using laminar flow patterning, Tollens' reagents were injected into a well-designed Y-junction microchannel that was 500 μm wide and 80 μm deep. Images of the deposited silver microheater with an applied flow velocity of 0.14 m s^{-1} were captured and measured every 20 s. The width of the deposited silver microheater at a fixed position increases rapidly initially, but then gradually slows after 2 min, as shown in figure 5(*a*). The maximum width of 28 μm can be achieved under this deposition condition in 3 min. The effect of the flow velocity on the deposited silver microheater width was also examined, as shown in figure 5(*b*). The width of the deposited silver microheater declined with an increase in the applied flow velocity. When a flow velocity of 0.7 m s^{-1} was applied, a silver microheater with a width of 12 μm was obtained at room temperature.

According to the experimental results, the apparition of the plateau for the width of deposited silver depends on the rate of Tollen's reaction, which is related to the concentration of chemical solutions and the deposition temperature only. Therefore, the time required to reach a plateau is independent of the flow rate applied in this study. A plateau of the growth in silver width is reached after 2 min, but the plateau of the growth of the silver thickness, equivalent to the thickness of the 200 μm high microchannel, is not yet reached. The silver microheaters were deposited in the microchannels after the anodic bonding process between silicon and Pyrex glass. Measuring the thickness of a deposited silver microheater during the silver deposition is difficult, although the etched depth should be equal to the height of the deposited silver. To estimate the deposition time required for deposited silver with target thickness, the microchannels were diced after the completion of the silver deposition. The thicknesses with different deposition times were measured on the cross-section of deposited silver. A minimum deposition time of 15 min is required to reach the target thickness of 200 μm at a flow rate of 0.08 m s^{-1}.

Various silver microstructure patterns can also be obtained by manipulating a continuous liquid stream. Multiple Y-junction microchannels were combined to generate multiple parallel laminar streams for silver wire deposition, as shown in figures 5(*c*) and (*d*). Multiple silver microstructures were obtained simultaneously without an additional MEMS fabrication process, such as microlithography or e-beam evaporation. This result can be used to create conductive structures inside a microchannel and provide high-aspect-ratio microheaters for the proposed device.

3.2. Sampling performance of micropreconcentrator

The GCs of the four prepared compounds with and without the adsorbent material were tested to evaluate their preconcentration efficiency, as shown in figure 6(*a*). The compound mixture was drawn through the preconcentrator at a flow rate of 3.5 mL min^{-1} for 600 s, which represents a total sampling volume of 35 mL. The peak widths at half height (PWHHs) of 3.75, 3.76, 4.26 and 5.92 s were examined for acetone, benzene, toluene and xylene, respectively. The sharp peaks of the four compounds indicate that the preconcentrated VOCs adsorbed to the adsorbent film inside the μPCT were desorbed completely without any residual compounds left within the adsorbent film. Typically, highly volatile compounds, such as acetone (vapor pressure 228.4 Torr), elute rapidly through the GC column; therefore, their PWHHs are determined primarily through desorption efficiency. Compounds with lower volatilities were retained on the GC column for longer durations; thus, the PWHHs of these compounds were determined by the retention behavior in the column, instead of the desorption efficiency of the μPCT.

Preconcentration factors were determined by calculating the ratio of the peak area of the μPCT with and without the adsorbent film. The desorption profiles of the four compounds injected by μPCT are shown in figures 6(*b*) to (*e*); the inset of each figure shows the signal without adsorbents. Preconcentration factors of 47 798, 38 346, 38 005 and 23 753 were obtained for acetone, benzene, toluene and xylene, respectively. Theoretically, the preconcentration factors of all tested VOCs should be similar under the same operating

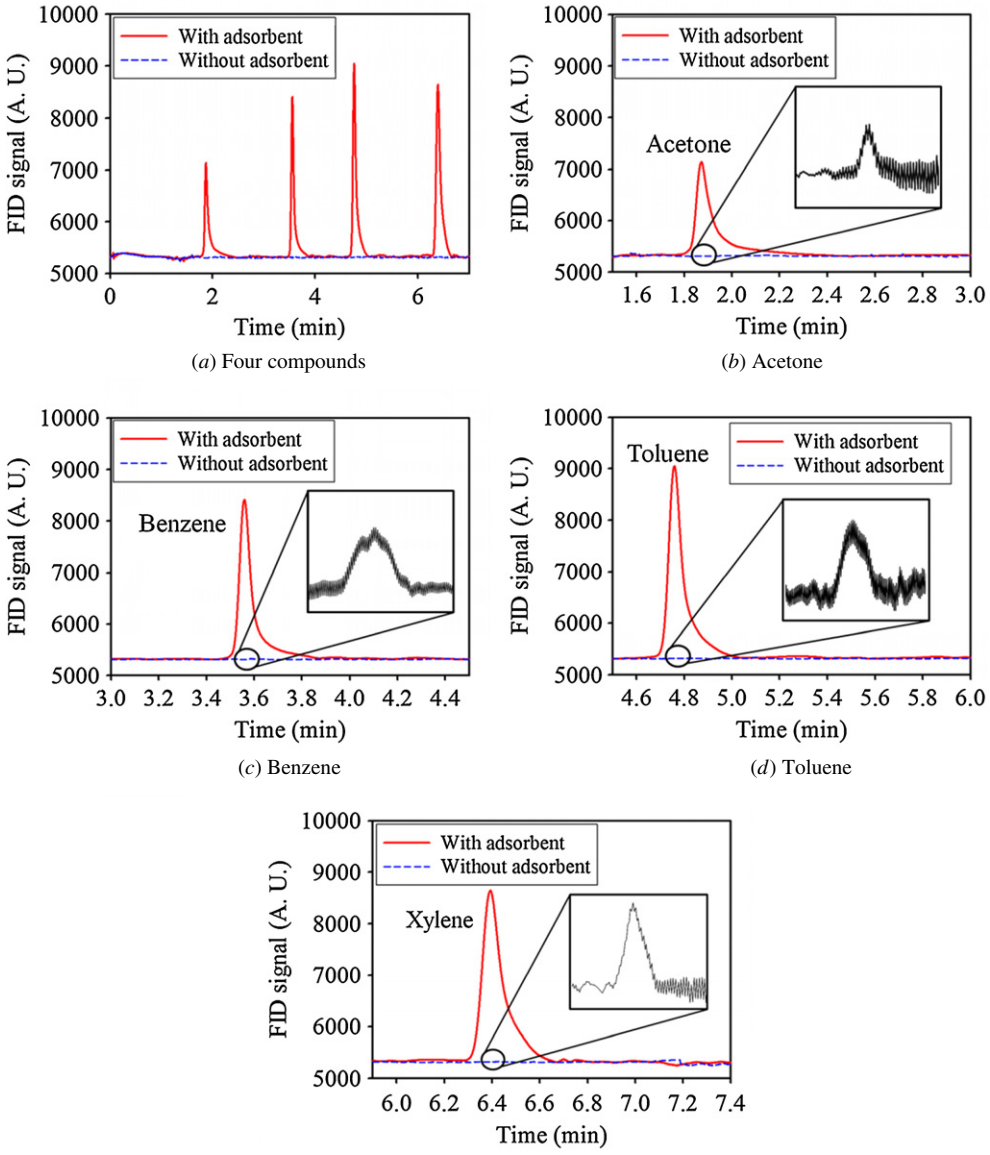

(*a*) Four compounds (*b*) Acetone

(*c*) Benzene (*d*) Toluene

(*e*) Xylene

Figure 6. A chromatogram of (*a*) four compounds; (*b*) acetone; (*c*) benzene; (*d*) toluene and (*e*) xylene, at a flow rate of 3.5 mL min^{-1} for 600 s with and without adsorbent material.

conditions. The preconcentration factors for benzene and toluene are relatively consistent. However, we believe that the unusually high preconcentration factor of acetone is caused by the uncertainty of measuring less-sensitive acetone at low concentrations. The relatively low preconcentration factor of xylene can be attributed to adsorption to the internal surface of μPCTs without adsorbent film. The surface roughness of channel walls, pillars and silver heaters allows retention of low-volatile xylene; therefore, the denominator for calculating the preconcentration factor was increased for xylene. The overall reduction of the preconcentration factor is reasonable.

To further evaluate the sampling capacity of μPCTs, sampling time was increased from 600 to 1800 s and tested under the same conditions. Table 1 shows the desorbed peak areas of the four separated compounds with two sampling times. The peak area under the FID signal curve of these four compounds increases proportionally, indicating that the collected sample does not differ significantly from the μPCT under our testing conditions.

Table 1. The peak area of four volatile organic compounds.

	Peak area			
Sampling time (s)	acetone	benzene	toluene	xylene
600	44.51	259.23	529.99	670.74
1800	118.29	716.69	1477.03	2017.31

Compared to the μPCT, the conventional preconcentrators are larger in size; therefore, the mass of adsorbent is much larger and requires external thermal desorption instruments to perform the desorption process. The advantages of our μPCT are lower power consumption, faster desorption and smaller in size than conventional preconcentrators. With these advantages, the μPCT typically provides a smaller

PWHH and a higher preconcentrator factor than conventional preconcentrators.

4. Conclusions

In this study, microfluidic laminar flow patterning was employed to deposit an in-channel silver microheater for a novel μPCT. The deposition conditions of the silver wire were optimized. Thick and high-surface-area silver wires, which can be formed in several minutes without employing sophisticated clean room processes, were used as heating elements. Integrated adsorbent formation was conducted using the pyrolysis technique. A highly porous carbon film was created as the adsorbent inside the μPCT to enable quantitative collection of VOCs. Four compounds were separated successfully using narrow PWHH (3.75 to 5.92 s). Preconcentration factors of >38 000 were observed for both benzene and toluene. This study presented a simple, rapid and cost-effective method for fabricating a novel μPCT for future μGC development.

Acknowledgments

This study was supported by the National Science Council of Taiwan, ROC, under the grant numbers NSC 100-2221-E-002-107-MY3 and NSC 100-2220-E-002-002.

References

[1] Kataoka H 1996 Derivatization reactions for the determination of amines by gas chromatography and their applications in environmental analysis *J. Chromatogr.* A **733** 19–34

[2] Poli D, Carbognani P, Corradi M, Goldoni M, Acampa O, Balbi B, Bianchi L, Rusca M and Mutti A 2005 Exhaled volatile organic compounds in patients with non-small cell lung cancer: cross sectional and nested short-term follow-up study *Respir. Res.* **6** 1–10

[3] Phillips M, Gleeson K, Hughes J M B, Greenberg J, Cataneo R N, Baker L and Mcvay W P 1999 Volatile organic compounds in breath as markers of lung cancer: a cross-sectional study *Lancet* **353** 1930–3

[4] Phillips M, Cataneo R N, Condos R, Erickson G A R, Greenberg J, Bombardi V L, Munawar M I and Tietje O 2007 Volatile biomarkers of pulmonary tuberculosis in the breath *Tuberculosis* **87** 44–52

[5] Hughes R C, Patel S V and Manginell R P 2000 A MEMS based hybrid preconcentrator/chemiresistor chemical sensor *Proc. 198th Meeting of the Electrochemical Society (22–27 Oct. 2000)* pp 142–50

[6] Agah M, Lambertus G R, Sacks R and Wise K D 2006 High-speed MEMS based gas chromatography *J. Microelectromech. Syst.* **15** 1371–8

[7] Lu C-J *et al* 2005 First-generation hybrid MEMS gas chromatograph *Lab Chip* **5** 1123–3

[8] Tian W-C, Pang S W, Lu C-J and Zellers E T 2003 Microfabricated preconcentrator-focuser for a microscale gas chromatograph *J. Microelectromech. Syst.* **12** 264–72

[9] Tian W-C, Chan H K L, Lu C-J, Pang S W and Zellers E T 2005 Multi-stage microfabricated preconcentrator-focuser for microscale gas chromatography system *J. Microelectromech. Syst.* **14** 498–507

[10] Lu C-J and Zellers E T 2001 A dual-adsorbent preconcentrator for a portable indoor-VOC microsensor system *Anal. Chem.* **73** 3449–57

[11] Serrano G, Chang H and Zellers E T 2009 A micro gas chromatograph for high-speed determinations of explosive vapors *Solid-State Sensors, Actuators and Microsystems Conf. (Transducers 2009) (21–25 June 2009)* pp 1654–7

[12] Alfeeli B and Agah M 2009 MEMS-Based selective preconcentration of trace level breath analytes *IEEE Sens. J.* **9** 1068–75

[13] Davis C E, Ho C K, Hughes R C and Thomas M L 2005 Enhanced detection of m-xylene using a preconcentrator with a chemiresistor sensor *Sensors Actuators* B **104** 2 207–16

[14] Ivanov P *et al* 2007 Improvement of the gas sensor response via silicon μ-preconcentrator *Sensors Actuators* B **127** 288–94

[15] Pijolat C, Camara M, Courbat J, Viricelle J-P, Briand D and de Rooij N F 2007 Application of carbon nano-powders for a gas micro-preconcentrator *Sensors Actuators* B **127** 179–85

[16] Roh S-C, Choi Y-M and Kim S-Y 2006 Sensitivity enhancement of a silicon micro-machined thermal flow sensor *Sensors Actuators* A **128** 1–6

[17] Lee S M, Dyer D C and Gardner J W 2003 Design and optimization of a high-temperature silicon micro-hotplate for nanoporous palladium pellistors *Microelectron. J.* **34** 115–26

[18] Briand D, Colin S, Gangadharaiah A, Vela E, Dubois P, Thiery L and de Rooij N F 2006 Micro-hotplates on polyimide for sensors and actuators *Sensors Actuators* A **132** 317–24

[19] Choi N-J, Lee Y-S, Kwak J-H, Park J-S, Park K-B, Shin K-S, Park H-D, Kim J-C, Huh J-S and Lee D-D 2005 Chemical warfare agent sensor using MEMS structure and thick film fabrication method *Sensors Actuators* B **108** 177–83

[20] Udrea F, Gardner J W, Setiadi D, Covington J A, Dogaru T, Lu C C and Milne W I 2001 Design and simulation of SOI CMOS micro-hotplate gas sensors *Sensors Actuators* B **78** 180–90

[21] Becker T, Mühlberger S, Barunmühl C B, Müller G, Meckes A and Benecke W 2000 Gas mixture analysis using silicon micro-reactor systems *J. Microelectromech. Syst.* **9** 478–84

[22] Kwon O J, Hwang S-M, Ahn J-G and Kim J J 2006 Silicon-based miniaturized-reformer for portable fuel cell applications *J. Power Sources* **156** 253–9

[23] Splinter A, Stürmann J, Bartels O and Benecke W 2002 Micro membrane reactor: a flow-through membrane for gas pre-combustion *Sensors Actuators* B **83** 169–74

[24] Geng X, Yuan H, Oguz H N and Prosperetti A 2001 Bubble-based micropump for electrically conducting liquids *J. Micromech. Microeng.* **11** 270–6

[25] Yin Z and Prosperetti A 2005 'Blinking bubble' micropump with microfabricated heaters *J. Micromech. Microeng.* 1683–91

[26] Martin M, Crain M, Walsh K, McGill R A, Houser E, Stepnowski J, Stepnowski S, Wu H-D and Ross S 2007 Microfabricated vapor preconcentrator for portable ion mobility spectroscopy *Sensors Actuators* B **126** 447–54

[27] Yeom J, Field C R, Bae B, Masel R I and Shannon M A 2008 The design, fabrication and characterization of a silicon microheater for an integrated MEMS gas preconcentrator *J. Micromech. Microeng.* **18** 12

[28] Ruiz A, Gràcia I, Sabaté N, Ivanov P, Sánchez A, Duch M, Gerbole M, Moreno A and Cané C 2007

Membrane-suspended microgrid as a gas preconcentrator for chromatographic applications *Sensors Actuators* A **135** 192–6

[29] Voiculescu I *et al* 2006 Micropreconcentrator for enhanced trace detection of explosives and chemical agents *IEEE Sensors J.* **6** 1094–104

[30] Alfeeli B, Jahromi M A Z and Agah M 2009 Micro preconcentrator with seedless electroplated gold as self-heating adsorbent *8th IEEE Conf. Sensors (25–28 Oct. 2009)* pp 1947–1950

[31] Kenis P J A, Ismagilov R F and Whitesides G M 1999 Microfabrication inside capillaries using multiphase laminar flow patterning *Science* **285** 83–5

[32] Formanek F, Takeyasu N and Tanaka T 2006 Selective electroless plating to fabricate complex three-dimensional metallic micro/nanostructures *Appl. Phys. Lett.* **88** 083110

[33] Tian W-C, Weigold J W and Pang S W 2000 Comparison of Cl_2 and F-based dry etching for high aspect ratio Si microstructures etched with an inductively coupled plasma source *J. Vac. Sci. Technol.* B **18** 1890–6